

# Thermopower in transition-metal perovskites

Wataru Kobayashi\*

*Division of Physics, Faculty of Pure and Applied Sciences,  
University of Tsukuba, Ibaraki 305-8571, Japan and*

*Tsukuba Research Center for Energy Materials Science (TREMS), University of Tsukuba, Ibaraki 305-8571, Japan*

High-temperature thermopower is interpreted as entropy that a carrier carries. Owing to spin and orbital degree of freedom, a transition metal perovskite exhibits large thermopower at high temperatures. In this paper, we revisit the high-temperature thermopower in the perovskites to shed light on the degree of freedom. Thus, we theoretically derive an expression of thermopower in one-dimensional octahedral-MX<sub>6</sub>-clusters chain using linear-response theory and electronic structure calculation of the chain based on the tight-binding approximation. The derived expression of the thermopower is consistent with the extended Heikes formula and well reproduced experimental data of several perovskite oxides at high temperatures. In this expression, a degeneracy of many electron states in octahedral ligand field (which is characterized by multiplet term) appears instead of the spin and orbital degeneracies. Complementarity in between our expression and the extended Heikes formula is discussed.

## I. INTRODUCTION

Transition-metal (M) oxides is one of fascinating quantum many-body systems, which exhibits Mott insulating state [1], spin-state crossover [2], peculiar magnetism accompanied by orbital ordering [3], high-temperature superconductivity [4], huge magneto-resistance [5], large thermopower [6], exotic superconductivity [7–9], multi-ferroicity [10], spin-orbit related Mott insulating state [11], spin frustration (possibly spin liquid) [12], and other relativistic effects such as Weyl semi metallic state [13]. A model material of the transition-metal oxides is a 3d-transition-metal perovskite oxides expressed as Ln<sub>1-x</sub>Ae<sub>x</sub>MO<sub>3</sub> (0 ≤ x ≤ 1, Ln: lanthanide, Ae: alkali earth metal, and O: oxygen.). This system has been extensively studied. In particular, metal-insulator (MI) transition was deeply understood in terms of filling, band-width, and dimensional controls [14]. The filling control is given by a substitution of Ae<sup>2+</sup> ion for Ln<sup>3+</sup> ion (hole doping). The band width ( $W$ ) is controlled by ionic radius ( $r_A$ ) of element at A site. Smaller  $r_A$  causes smaller M-O-M bond angle, which realizes smaller  $W$ . Tolerance factor ( $\tau$ ) is a function of  $r_A$  and a measure of strain in the perovskite structures. For  $\tau \sim 0.9 - 1.0$ , cubic structure with M-O-M bond angle of 180° realizes. With decreasing  $r_A$  as La<sup>3+</sup> → Pr<sup>3+</sup> → ... → Y<sup>3+</sup> → Lu<sup>3+</sup>, and Ba<sup>2+</sup> → Sr<sup>2+</sup> → Ca<sup>2+</sup>,  $\tau$  decreases which causes decrease in  $W$ .  $\frac{U}{W}$  ( $U$ : on-site coulomb interaction) is a key parameter, which gives a quantum critical point of the metal-insulator transition (MIT). Revealing electronic structures in the 3d-transition-metal perovskite oxides is generally difficult because of the electron correlation. Hubbard model [15] is a well known model that duplicates the MIT in the strongly correlated system [14, 16].

Thermopower ( $S$ ) is a phenomenological transport coefficient, and is defined as a temperature ( $T$ ) deriva-

tive of thermoelectric voltage ( $V$ ) as  $S \equiv \frac{dV}{dT}$ , and can be applied for thermoelectric energy conversion [17]. Thermopower at high-temperature limit in the quantum many-body systems is interpreted as entropy that a carrier carries in a regime of linear response theory with the Hubbard model [18, 19]. Chaikin and Beni generalized Heikes formula [18] to explain thermopower of interacting Fermi systems with spin, and explained thermopower of strongly correlated p-electron system (one-dimensional organic conductor) with spin entropy term  $-\frac{k_B}{e} \ln 2$  [19]. Further, Doumerc extended the formula to apply for a system containing a mixed valent cation M<sup>n+</sup>/M<sup>(n+1)+</sup> using spin multiplicity (2S<sub>n</sub> + 1) [20]. Marsh and Parris again extended the formula to take into account the orbital degeneracy, and qualitatively explained thermopower of LaCrO<sub>3</sub>[21], LaMnO<sub>3</sub>[22] and their related perovskite systems. Koshibae *et al.* also explained the large thermopower of NaCo<sub>2</sub>O<sub>4</sub> using the spin and orbital degrees of freedom and proposed application of their theory to Co perovskite oxides [23]. In their theories, such degrees of freedom is introduced by counting a number of cases in many electrons configuration in e<sub>g</sub> and t<sub>2g</sub> orbitals, and they seem to work well. To further consider the degrees of freedom, we derive a similar formula constructed from many electron states in MX<sub>6</sub> cluster with octahedral ligand (X: ligand element) field without a use of one-band Hubbard model.

In this paper, we construct thermopower of one-dimensional MX<sub>6</sub>-clusters chain model targeting the 3d-transition-metal perovskite oxides with  $\frac{U}{W} \gg 1$ . In a derived expression of the thermopower, we find that a degeneracy of many-electron states in the MX<sub>6</sub>-cluster is included instead of the degeneracies of spin and orbital. We will discuss the relation between spin and orbital degrees of freedom and the degeneracy of the many-electron states. We further apply our formula to experimental data of several 3d-transition-metal perovskite oxides. Lastly, effects of spin-orbit interaction and Jahn-Teller distortion on the thermopower will be discussed in the section of III. B.

\* kobayashi.wataru.gf@u.tsukuba.ac.jp

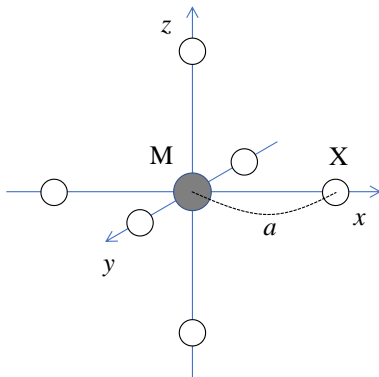


FIG. 1. (Color online) Schematic figure of  $\text{MX}_6$  octahedron with  $O_h$  symmetry. White circle represents a ligand (X) with its charge is  $-Ze$  ( $Z$ : positive integer,  $e$ : charge unit). d electrons in 3d transition metal element (M) feel octahedral ligand field.

## II. METHODS

In this section, first, we briefly review the crystal (ligand) field theory. We see many d-electron states in octahedral ligand field, term symbol, and how to count a degeneracy of the states that is represented by the term symbol. Second, we explain the tight-binding approximation (molecular-orbital theory) for the construction of the electronic structure of periodically aligned one-dimensional  $\text{MX}_6$ -clusters chain system (hereafter, clusters-chain model. See Fig. 2). Third, we derive an expression of thermopower at high-temperature limit for the clusters-chain model, in a regime of linear-response theory. Last, we discuss complementarity in between the extended Heikes formula and our expression.

### A. Crystal field theory (CFT)

To calculate physical properties of solids, we generally need to treat its electronic structure correctly taking into account periodicity of the crystal. However, if on-site coulomb interaction ( $U$ ) is much larger than inter-atomic transfer integral ( $t$ ), we may discuss the physical properties of the crystal based on the atomic electronic states. Effects from other atoms can be treated as crystal field or ligand field which includes hybridization with p-orbitals of the ligands.

Here, we briefly review the crystal field theory (CFT). CFT describes a breaking of a degeneracy of electron orbital states (d or f orbital states) of atom (or ion) due to a static electric field produced by a surrounding charge distribution. Suppose d-electrons of the atom (or the ion) are surrounded by 6 negative charges ( $-Ze$ ,  $Z$ : positive integer,  $e$ : charge unit) at  $\mathbf{R}_k = (a, 0, 0)$ ,  $(0, a, 0)$ ,  $(0, 0, a)$ ,  $(-a, 0, 0)$ ,  $(0, -a, 0)$ , and  $(0, 0, -a)$ . Then, the Hamiltonian ( $H_n$ ) of the  $n$  d-electrons ( $n$ : a number of

d-electrons) is described as

$$H_n = \left( \sum_{i=1}^n \frac{\mathbf{p}_i^2}{2m_e} + v_{\text{core}}(r_i) + v_{\text{CF}}(r_i) \right) + \sum_{j>i=1}^n \frac{e^2}{r_{i,j}}, \quad (1)$$

where  $m_e$ ,  $\mathbf{p}_i$ ,  $r_i = |\mathbf{r}_i|$ , and  $r_{i,j} = |\mathbf{r}_i - \mathbf{r}_j|$  represent electron mass, momentum of  $i$ -th electron, distance in between a position of  $i$ -th electron and the origin, and relative distance in between  $\mathbf{r}_i$  and  $\mathbf{r}_j$ .  $v_{\text{core}}(r_i)$  is a potential of atom and valence electrons (central force field approximation),  $v_{\text{CF}}(r_i)$  is a crystal field,  $v_{\text{CF}}(r_i) = \sum_{k=1}^6 \frac{Ze^2}{|\mathbf{R}_k - \mathbf{r}_i|}$ , and the last term represents electron interaction between d electrons. When  $n = 1$ , the fourth term vanishes which results in well known  $d_{x^2-y^2}$  (we denote this as  $\phi_v$  or  $v$ ),  $d_{3z^2-r^2}$  ( $\phi_u$  or  $u$ ),  $d_{xy}$  ( $\phi_\zeta$  or  $\zeta$ ),  $d_{yz}$  ( $\phi_\xi$  or  $\xi$ ), and  $d_{zx}$  ( $\phi_\eta$  or  $\eta$ ) wave functions are obtained. Note that these wavefunctions are real functions. For  $v_{\text{core}}(r_i) = -\frac{e^2}{r_i}$ , energy gap in between  $e_g$  and  $t_{2g}$  orbitals is evaluated as  $10Dq$ , where  $D = \frac{35Ze}{4a^5}$  and  $q = \frac{2e}{105}\langle r^4 \rangle$  (average of  $r^4$ ,  $\langle r^4 \rangle \equiv \int |R_{nd}|^2 r^4 r^2 dr$ ,  $R_{nd}$  is radial wavefunction of  $nd$  states.) [24]. Parameters  $Z$  and  $a$  can tune the energy gap. In this sense,  $Z$  and  $a$  can express material's characteristics. Thus, under octahedral coordination, 5-fold d orbitals split into 3-fold  $t_{2g}$  and 2-fold  $e_g$  orbitals.

When  $n > 1$ , electron correlation should be taken into account. Tanabe and Sugano have constructed solutions for  $n$  d-electrons ( $1 \leq n \leq 9$ ) in the crystal field (strong crystal field limit) [25, 26]. As a result, the many-electron state is found to be expressed as a linear combination of Slater determinants including  $\phi_u$  (or  $u$ ),  $\phi_v$  ( $v$ ),  $\phi_\zeta$  ( $\zeta$ ),  $\phi_\xi$  ( $\xi$ ),  $\phi_\eta$  ( $\eta$ ) (spin up),  $\bar{\phi}_u$  (or  $\bar{u}$ ),  $\bar{\phi}_v$  ( $\bar{v}$ ),  $\bar{\phi}_\zeta$  ( $\bar{\zeta}$ ),  $\bar{\phi}_\xi$  ( $\bar{\xi}$ ),  $\bar{\phi}_\eta$  ( $\bar{\eta}$ ) (spin down). Write the many-electron state as  $\Phi_n(t_2^p e_g^q : 2S+1 \Gamma M_o \gamma)$ , where  $p$  and  $q$  ( $n = p + q$ ) represent a number of electrons at  $t_2$  orbitals ( $\zeta, \eta, \xi$ ) and  $e$  orbitals ( $u, v$ ),  $2S+1 \Gamma$  represents multiplet term,  $M_o$  is a quantum number of total orbital angular momentum, and  $\gamma$  represents ground function of irreducible representation  $\Gamma$  (e.g.  $\Gamma = T_2$ ,  $\gamma = \xi, \eta, \zeta$ ). As an example, we briefly treat  $n = 2$ . A number of cases for  $(t_2)^2$  configuration is 15 ( $= {}_6C_2$ ). Thus, we can provide 15 Slater determinant as  $|\xi\eta\rangle$ ,  $|\bar{\xi}\bar{\eta}\rangle$ ,  $\dots$ , and  $|\xi\bar{\xi}\rangle$ . Then, using a linear combination ( $\Phi_2$ ) of these 15 Slater determinants,  $\langle \Phi_2 | \frac{e^2}{r_{i,j}} | \Phi_2 \rangle$  can be diagonalized, then we obtain  $\Phi_2 = \Phi_2(t_2^2 : 2S+1 \Gamma M_o \gamma)$ . This solution is further characterized by multiplet term which represents symmetry of the many-electron states under octahedral ligand field. For example,  $\Phi_2(t_2^2 : {}^3T_1 M_o = 1\gamma) = |\xi\eta\rangle$ ,  $|\eta\zeta\rangle$ , and  $|\zeta\xi\rangle$ .  $\Phi_2(t_2^2 : {}^3T_1 M_o = 0\gamma) = \frac{1}{\sqrt{2}} \{|\xi\bar{\eta}\rangle - |\eta\bar{\xi}\rangle\}$ ,  $\frac{1}{\sqrt{2}} \{|\eta\bar{\zeta}\rangle - |\zeta\bar{\eta}\rangle\}$ , and  $\frac{1}{\sqrt{2}} \{|\zeta\bar{\xi}\rangle - |\xi\bar{\zeta}\rangle\}$ .  $\Phi_2(t_2^2 : {}^3T_1 M_o = -1\gamma) = |\bar{\xi}\bar{\eta}\rangle$ ,  $|\bar{\eta}\bar{\zeta}\rangle$ , and  $|\bar{\zeta}\bar{\xi}\rangle$ . These 9 functions are energetically degenerated. A degeneracy of the multiplet term  $2S+1 \Gamma$  is a product of spin multiplicity ( $2S+1$ ) and  $\Gamma_0$ .  $\Gamma_0$  is a dimensional number of irreducible representation (1 for A(B), 2 for E, and 3 for T). Thus, a degeneracy of  ${}^3T_1$  is expressed as  $3 \times 3 = 9$ .



$d^n$	electronic configuration	spin state	ground multiplet term ( $^{2S+1}\Gamma$ )	degeneracy of $^{2S+1}\Gamma$ ( $\Gamma$ )
$d^0$	$(t_{2g})^0(e_g)^0$	-	$^1A_{1g}$	1
$d^1$	$(t_{2g})^1(e_g)^0$	-	$^2T_{2g}$	6
$d^2$	$(t_{2g})^2(e_g)^0$	-	$^3T_{1g}$	9
$d^3$	$(t_{2g})^3(e_g)^0$	-	$^4A_{2g}$	4
$d^4$	$(t_{2g})^3(e_g)^1$	high spin	$^5E_g$	10
	$(t_{2g})^4(e_g)^0$	low spin	$^3T_{1g}$	9
$d^5$	$(t_{2g})^3(e_g)^2$	high spin	$^6A_{1g}$	6
	$(t_{2g})^4(e_g)^1$	*intermediate spin	$^*4T_{1g}$	12
	$(t_{2g})^5(e_g)^0$	low spin	$^2T_{2g}$	6
$d^6$	$(t_{2g})^4(e_g)^2$	high spin	$^5T_{2g}$	15
	$(t_{2g})^5(e_g)^1$	*intermediate spin	$^*3T_{1g}$	9
	$(t_{2g})^6(e_g)^0$	low spin	$^1A_{1g}$	1
$d^7$	$(t_{2g})^5(e_g)^2$	high spin	$^4T_{1g}$	12
	$(t_{2g})^6(e_g)^1$	low spin	$^2E_g$	4
$d^8$	$(t_{2g})^6(e_g)^2$	-	$^3A_{2g}$	3
$d^9$	$(t_{2g})^6(e_g)^3$	-	$^2E_g$	4
$d^{10}$	$(t_{2g})^6(e_g)^4$	-	$^1A_{1g}$	1

TABLE I. Number of d electrons ( $d_n$ ), electronic configuration, spin state, ground multiplet term ( $^{2S+1}\Gamma$ ), and degeneracy of  $^{2S+1}\Gamma$  ( $\Gamma$ ). The ground terms were referred from Ref[26]. \* : these intermediate states are excited states in Tanabe-Sugano diagram.

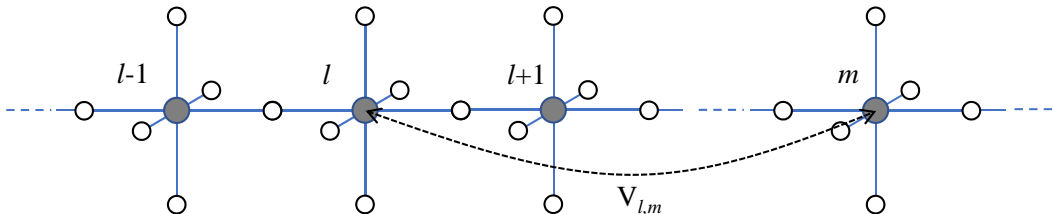


FIG. 2. (Color online) Schematic figure of periodically aligned one-dimensional N-clusters chain. The broken arrow represents inter-cluster interaction in between  $l$ -th and  $m$ -th clusters ( $V_{l,m}$ ).

When a material can be well described as band picture (mean-field approximation), the Boltzmann equation regime works well. Based on the band calculation and the Boltzmann equation, Singh reproduced a large thermopower ( $\sim 110 \mu\text{V/K}$ ) of  $\text{NaCo}_2\text{O}_4$  at 300 K [28]. Even if band picture does not work well (ex. correlated hopping conduction), by carefully taken into account interactions in a Hamiltonian, Kubo-Luttinger formalism [29, 30] works well. Recently, Matsuura *et al.* explained large thermopower of ( $\sim 20 \text{ mV/K}$ ) at around 10 K taking into account electron-phonon interaction [31]. Thermopower of strongly correlated electron system including 3d transition metal perovskite oxide has been qualitatively explained based on single-band Hubbard model [21–23]. And introduced degeneracies of spin and orbital plays an important role. To further consider the degrees of freedom, we evaluate the thermopower of the one-dimensional N-clusters chain.

First, we consider the term  $\frac{1}{k_B T} \left( \frac{J_q}{J} \right)$ .  $\left( \frac{J_q}{J} \right)$  is an averaged energy that a carrier carries. For our model, against an external field [such as electric field  $E$  or temperature gradient ( $\nabla T$ )] as perturbation, most of the initial states excites within the band width  $W$ . So that we may eval-

uate  $\frac{1}{k_B T} \left( \frac{J_q}{J} \right)$  as  $\sim \frac{W}{k_B T}$ . Thus, for  $W \ll k_B T \ll U$ , at the limit of  $T \rightarrow \infty$ ,

$$\lim_{T \rightarrow \infty} S = \frac{\mu}{eT} = -\frac{1}{e} \left( \frac{\partial s}{\partial N_e} \right)_{E,V}, \quad (6)$$

where,  $s$ ,  $N_e$ ,  $E$ , and  $V$  represents entropy, electron number, energy and volume in the N-clusters chain, respectively. We call this high-temperature limit value. According to the  $t - J$  model by Koshibae and Maekawa [32], the high-temperature limit value is almost realized at around  $\frac{k_B T}{t} \sim 5$ . According to one-dimensional Hubbard model analysis,  $S$  almost saturates at around  $\frac{k_B T}{t} \sim 1$  [33]. This is also consistent with assumption of our method [ $\left( \frac{J_q}{J} \right) \sim W$ ].

When  $V_{l-1,l}$  and  $V_{l,l+1} \sim W$ , although all the eigenstates and eigenvalues of the N-clusters chain system are exactly determined, calculation of the entropy (counting of a number of degenerated eigenstates at total energy  $E$ ) is highly complicated. Thus, we consider the limit of  $W \rightarrow 0$  (Namely  $V_{l,m} \rightarrow 0$ ). At the  $W = 0$  limit, the N-clusters chain system becomes simple, namely a periodically-aligned one-dimensional noninteracting clusters. Then, the wavefunction of the system is described

as a direct product of the wavefunction of the  $l$ -th cluster  $[\Phi_{n_{il}}(t_2^p e^q : ^{2S+1} \Gamma M_o \gamma)]$ ,

$$\Psi_N = \prod_{l=1}^N \Phi_{n_{il}}(t_2^p e^q : ^{2S+1} \Gamma M_o \gamma). \quad (7)$$

Total energy  $E$  of the system is expressed as  $E = (N - M)E_3 + ME_4$ . A number of electrons  $N_e$  is expressed as  $N_e = (N - M)n_3 + Mn_4$ , where  $n_3$  ( $n_4$ ) represents a number of electrons in a cluster with  $M^{3+}$  ( $M^{4+}$ ). Since  $n_3 - n_4 = 1$ ,  $N_e$  becomes  $N_e = Nn_3 - M$ . Then, a number ( $g$ ) of degenerated eigenstates at  $E$  is evaluated as

$$g = \Gamma_3^{N-M} \Gamma_4^M \frac{N!}{M!(N-M)!}, \quad (8)$$

where  $\Gamma_3$  ( $\Gamma_4$ ) represents degeneracy of many-electron states in a  $M^{3+}$  ( $M^{4+}$ ) cluster at  $E_3$  ( $E_4$ ). Using Boltzmann principle of entropy  $s = k_B \ln g$ , thermopower at the high-temperature limit becomes

$$S = -\frac{k_B}{e} \left( \frac{\partial \ln g}{\partial N_e} \right)_{E,V} = \frac{k_B}{e} \left( \frac{\partial \ln g}{\partial M} \right)_{E,V}. \quad (9)$$

By substituting Eq. 8 to Eq. 9 and using Stirling's approximation,

$$S = -\frac{k_B}{e} \ln \left( \frac{\Gamma_3}{\Gamma_4} \frac{x}{1-x} \right), \quad (10)$$

is obtained as a final formula where  $x$  is defined as  $\frac{M}{N}$ .

#### D. Comparison with the extended Heikes formula

The extended Heikes formula expresses thermopower in  $d$  electron system [20–23]. The total number of configurations for  $t \ll k_B T \ll U$  will be written as

$$g = g_3^{N_A - M} g_4^M \frac{N_A!}{M!(N_A - M)!}, \quad (11)$$

where  $N_A$  is a system size,  $M$  is the number of  $M^{4+}$  ions.  $g_3$  and  $g_4$  are defined as number of electronic configurations of  $M^{3+}$  and  $M^{4+}$  ions (spin and orbital degrees of freedom). Substituting Eq. 11 for Eq. 9, then, the thermopower is obtained as

$$S = -\frac{k_B}{e} \ln \left( \frac{g_3}{g_4} \frac{x}{1-x} \right), \quad (12)$$

where  $x$  is a ratio of  $M^{4+}$  ion to the system size  $N_A$  ( $x = \frac{M}{N_A}$ ) [21–23]. Eqs. 11 and 12 are almost identical to Eqs. 8 and 10.

Now let us compare  $g_i$  with  $\Gamma_i$  ( $i = 3, 4$ ). According to Marsh, Parris, and Koshibae *et al.*, [21–23], a number of  $n$   $d$ -electrons configurations in  $e_g$  and  $t_{2g}$  orbitals with use of spin multiplicity ( $2S + 1$ ) and orbital degeneracy is calculated using a number of cases. When

$t_{2g}$  or  $e_g$  orbital is partially occupied, direct product of totally symmetric representation and irreducible representation becomes  ${}^1A_{1g} \times {}^{2S+1}\Gamma = {}^{2S+1}\Gamma$ . So that degeneracy of orbital can be dimension of  $\Gamma$  ( $\Gamma = A$  or  $B \rightarrow 1, E \rightarrow 2, T \rightarrow 3$ ). Thus, degeneracy of the ground multiplet term becomes equal to degeneracies of spin and orbital. However, if both  $e_g$  and  $t_{2g}$  orbitals are partially occupied (e.g. excited state such as intermediate spin state of  $\text{Co}^{3+}$ ), product of representations becomes  $E_g \times T_{2g} = T_{1g} + T_{2g}$  in  $O_h$  symmetry. Then, the number of the configuration differs from the degeneracies of spin and orbital [e.g.  $t_{2g}^4 e_g^1$  ( $S = \frac{3}{2}$ )  $\rightarrow$  spin multiplicity is 4, orbital degeneracy is 3 for  $t_{2g}$ , 2 for  $e_g$ , thus degeneracies of spin and orbital becomes 24 [23].] because coulomb interaction split 24 states into 12 + 12 states depending on the symmetry of the many electron states. However, if these states are regarded as degenerated due to some ignored interaction in the crystal field approximation [23],  $g_i$  becomes identical to  $\Gamma_i$  for  $0 \leq n \leq 10$ .

Next, we see a difference of the derivations. Marsh and Parris calculated chemical potential with use of “grand canonical ensemble” [21, 22]. Koshibae *et al.*, calculated the chemical potential with use of “micro canonical ensemble” [23]. Since different ensembles lead the same expression, the extended Heikes formula is validly constructed based on thermodynamics and quantum statistical mechanics. Our formula is consistent with their results as shown above. We derived our expression of  $S$  by considering micro canonical ensemble of exact many-electron states at total energy  $E$ . Since the extended Heikes formula and our formula are almost identical, these formulae are complementary.

Thanks to the comparison shown above, now we recognize an important feature. When thermopower of the metallic perovskite with magnetic interaction is discussed, the Heikes formula has an advantage to guess the degeneracy of the many electron states. Since it is highly difficult to exactly know the eigenstates and the eigenvalues of correlated metallic states ( $U \ll k_B T$ ), our method is not applicable. Thus, thermopower in correlated metallic state even seems to be reproduced by the spin and orbital degeneracies.  $S$  at high temperature limit is entropy that a carrier carries. So that the experimental data at high temperatures gives an important information about the entropy. The extended Heikes formula is also applicable for even frustrated state with triangular lattice.

### III. COMPARISON WITH EXPERIMENTS AND DISCUSSION

As shown in the introduction, a condition,  $W \ll k_B T \ll U$  is realizing in 3d-transition-metal perovskite with low  $\tau$  (small  $W$ ) [14]. At  $V_{i,m} \sim 0$  ( $W \ll k_B T$ ), many of the system exhibit paramagnetic insulating state. Thus, 3d transition metal perovskite with insulating (semiconducting) conductivity due to hopping con-

duction and para magnetism will exhibit almost saturated thermopower at high temperatures. We investigate  $x$  dependence of thermopower at high temperatures from previous works in which the material satisfies this condition. Now, let's compare experimental data with our expression. (Note that the proper data are not found after  $d^7$  in the literature.)

### A. $d^0/d^1$ system

$d^0/d^1$  system corresponds to  $Ti^{4+}/Ti^{3+}$  system.  $SrTiO_3$  is a band insulator, and with La doping (electron doping),  $Sr_{1-x}La_xTiO_3$  ( $0.0 \leq x \leq 0.1$ ) exhibits paramagnetic metallic states. Thermopower of the system exhibits negatively large value, which is highly expected as a n-type thermoelectric material [34]. With  $La^{3+} \rightarrow Pr^{3+}$ ,  $Pr_{1-x}Sr_xTiO_3$  exhibits insulating state possibly due to narrower  $W$  than that of  $La_{1-x}Sr_xTiO_3$ .

Figure 3(a) shows  $x$  dependence of thermopower in  $Pr_{1-x}Sr_xTiO_3$  ( $0.7 \leq x \leq 0.98$ ) at 1200 K [35]. With  $\Gamma_3 = 6$  and  $\Gamma_4 = 1$ , Eq. 10 is drawn as a broken line. The  $x$  dependence of the thermopower is referred from the Fig. 5 in Ref. [35]. They still gradually increase even at 1200 K due to rather large  $W$  of this system. However, the thermopower data seem to saturate at higher temperatures. So that we plot these data in Fig. 3(a)

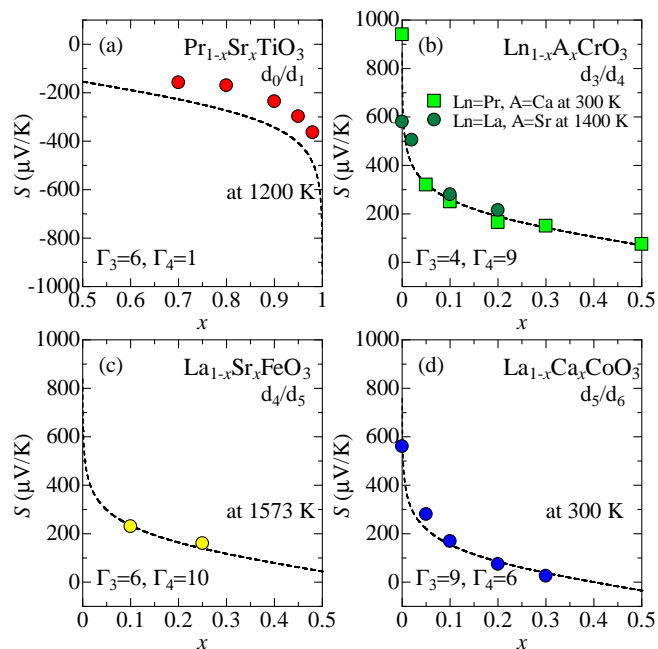


FIG. 3. (Color online)  $x$  dependence of thermopower in (a)  $d_0/d_1$ -system  $Pr_{1-x}Sr_xTiO_3$  at 1200 K, (b)  $d_3/d_4$ -systems  $La_{1-x}Sr_xCrO_3$  at 1400 K and  $Pr_{1-x}Ca_xCrO_3$  at 300 K, (c)  $d_4/d_5$ -system  $La_{1-x}Sr_xFeO_3$  at 1573 K, and (d)  $d_5/d_6$ -system  $La_{1-x}Ca_xCoO_3$  at 300 K. In each figure of (a)-(d), Eq. 10 is drawn as a broken line. Numbers of  $\Gamma_3$  and  $\Gamma_4$  are displayed in the each figure.

with the theoretical curve.

### B. $d^1/d^2$ system

The filling controlled Mott transition system  $La_{1-x}Sr_xVO_3$ [36]. is a typical  $d^1/d^2$  system ( $V^{4+}/V^{3+}$  system). According to the schematic metal-insulator diagram in Fig. 65 of Ref. [14], this system has rather large  $W$ . So that thermopower of this system does not indicate its saturation (they exhibit strong  $T$ -dependence) even at high temperatures (1250 K). Thus, our expression can not treat this result. Combining the extended Heikes formula and dynamical mean field theory (DMFT) calculation on the single-band Hubbard model, M. Uchida *et al.*, indicate that the thermopower merge a value expected by the Heikes formula for  $U \ll k_B T$  limit at high temperatures.

### C. $d^2/d^3$ system

$La_{1-x}Sr_xCrO_3$  is a typical  $d^2/d^3$  system ( $Cr^{4+}/Cr^{3+}$  system) which exhibits insulating  $T$  dependence, and its thermopower almost saturates above 1000 K [37].  $Pr_{1-x}Ca_xCrO_3$ [38] has a narrower  $W$  than that of  $La_{1-x}Sr_xCrO_3$ . The thermopower of this system almost saturate above 250 K. And paramagnetic insulating state is realized above 250 K. Pal *et al.*, has shown that the  $x$  dependence of the thermopower is qualitatively explained by the extended Heikes formula. Marsh and Parris reproduced thermopower of  $La_{1-x}Sr_xCrO_3$ [21] system at 1400 K by using their theory with degeneracies of spin and orbital  $\beta_0 = 9$ , and  $\beta_1 = 4$ . In Fig. 3(b), we replotted the data of  $La_{1-x}Sr_xCrO_3$  [37] and  $Pr_{1-x}Ca_xCrO_3$  [38] with Eq. 10.

### D. $d^3/d^4$ system

$La_{1-x}Sr_xMnO_3$ [22], and  $La_{1-x}Ca_xMnO_3$ [22] are the typical model materials of  $d^3/d^4$  system ( $Mn^{4+}/Mn^{3+}$  system). From extensive research of these systems, a rich phase diagram is obtained. Charge ordering, ferromagnetism due to strong magnetic coupling, Jahn-Teller instability and phase separation cause the rich phases. Marsh and Parris explained the  $x$  dependence of the thermopower of these systems using their theory [22]. It seems to us that in particular,  $\Gamma_0 = 1$  ( $\Gamma_0$ : spin degeneracy) due to long-range magnetic coupling and  $\Delta_{JT} \ll k_B T$ ,  $U \ll k_B T$  cause weak  $x$  dependence of the thermopower below  $x = 0.2$ . Palstra *et al.*, also reported  $x$  dependence of the thermopower for  $La_{1-x}Ca_xMnO_3$ , and found almost  $x$  independent values at 475 K [39]. Kobayashi *et al.*, reported  $x$  dependence of the thermopower of  $CaMn_{3-x}Cu_xMn_4O_{12}$  with narrower M-O-M bond angle ( $= 142^\circ$ ), and found almost  $x$  independent

values at 1373 K [40]. They exhibit insulating  $T$  dependence of electrical conductivity possibly due to narrow band width  $W$ . However, Jahn-Teller instability and short- and long-range magnetic interaction seems to cause the small almost  $x$  independent thermopower.

### E. $d^4/d^5$ system

$\text{La}_{1-x}\text{Sr}_x\text{FeO}_3$ [41] is a typical  $d^4/d^5$  system ( $\text{Fe}^{4+}/\text{Fe}^{3+}$  system).  $\text{La}_{1-x}\text{Sr}_x\text{FeO}_3$  ( $x = 0.1$  and  $0.25$ ) exhibit paramagnetic insulating state [14]. The thermopower almost saturate for  $x = 0.1$  above 1173 K. We plotted the data at 1573 K with  $\Gamma_3 = 6$  and  $\Gamma_4 = 10$  (for high spin) in Fig. 3(c).

### F. $d^5/d^6$ system

$\text{LaCoO}_3$  is well-known as a spin-state crossover system [2]. With Sr doping, the system experiences MIT and shows ferromagnetic metallic state. Co-O-Co bond angle is smaller for  $A = \text{Ca}$  than that for  $A = \text{Sr}$ .  $\text{La}_{1-x}\text{Sr}_x\text{CoO}_3$ [42, 43] is a typical  $d^5/d^6$  system ( $\text{Co}^{4+}/\text{Co}^{3+}$  system), and exhibits insulating temperature dependence of resistivity up to  $x = 0.3$  although it's  $x = 0.2$  for  $\text{La}_{1-x}\text{Ca}_x\text{CoO}_3$ . The thermopower seems to saturate around 300 K. (Note that at higher temperatures this system exhibits temperature induced MIT. Toward the MIT,  $S$  decreases with  $T$ .) We replotted the thermopower data at 300 K in  $\text{La}_{1-x}\text{Ca}_x\text{CoO}_3$ [43] with  $\Gamma_3 = 9$  and  $\Gamma_4 = 6$  (intermediate state for  $\text{Co}^{3+}$ , low spin state for  $\text{Co}^{4+}$ ) in Fig. 3(d).

### G. general discussion

As shown above, our formula well reproduces the thermopower of 3d transition metal perovskite oxides with small  $W$  and large  $U$  without both short- and long-range magnetic coupling. Although the extended Heikes formula seems to be applicable even for the correlated metallic state with magnetic interaction at a limit of  $U \ll k_B T$  (for  $\text{V}^{4+}/\text{V}^{3+}$ , and  $\text{Mn}^{4+}/\text{Mn}^{3+}$  systems). In

general, these conditions give weak  $x$  dependence of the thermopower and rather small  $S$  value due to small spin degree of freedom ( $\sim 1$ ). Thus, entanglement in between other clusters works to decrease the thermopower. Jahn-Teller effect and spin orbit interaction can also be treated within our regime beyond the present evaluation. For example,  $\text{La}_{1-x}\text{Ca}_x\text{MnO}_3$  has Jahn-Teller instability. The distortion of the  $\text{MO}_6$  octahedron induces  ${}^5\text{E}_g \rightarrow {}^5\text{A}_{1g} + {}^5\text{B}_{1g}$ , namely 10-fold degeneracies becomes 5-fold degeneracies with energetically stable state and 5-fold degeneracies with unstable state. This effect is treated as  $\Gamma_3 = 10 \rightarrow 5$  for  $d^4/d^5$  system. As shown here, these effects break the degeneracy of the many electron states at any energy  $E$ , which gives smaller  $S$  values than that the present one.

## IV. CONCLUSION

In conclusion, we widely investigate thermopower (at high temperatures) of 3d transition metal perovskite oxides comparing the extended Heikes formula. We constructed an expression of the thermopower from many electron electronic states of  $\text{MX}_6$  (M: transition metal, X: ligand element) octahedral clusters and reproduced  $x$ -dependence of the thermopower of several perovskites with  $W \ll k_B T \ll U$  using a degeneracy of many electron states that multiplet term represents at the total energy  $E$ . Comparison of our expression with the extended Heikes formula, complementarity of these formulae become clear. Thermopower in correlated metallic state with small  $U$  and the magnetic coupling can be treated by the extended Heikes formula. This is highly efficient because without knowing the exact many electron states, we can evaluate thermopower with considering the inner degrees of freedom. Even in transport, we see an importance of crystal symmetry, which regulates a value of thermopower.

## ACKNOWLEDGMENTS

I would like to thank H. Kobayashi and S. Kobayashi for their supports.

- 
- [1] N. F. Mott, The basis of the electron theory of metals, with special reference to the transition metals, Proc. Phys. Soc. A **62**, 416 (1949).
  - [2] J. B. Goodenough, An interpretation of the magnetic properties of the perovskite-type mixed crystals  $\text{La}_{1-x}\text{Sr}_x\text{CoO}_{3-\lambda}$ , J. Phys. Chem. Solids **6**, 287 (1958).
  - [3] K. I. Kugel and D. I. Khomskii, The Jahn-Teller effect and magnetism: transition metal compounds, Soviet Physics Uspekhi. **25**, 231(1982).
  - [4] J. B. Bednorz and K. A. Muller, Possible high  $T_c$  superconductivity in the Ba-La-Cu-O system, Zeitschrift fur Physik B Condensed Matter **64**, 189 (1986).
  - [5] Y. Tokura, A. Urushibara, Y. Moritomo, T. Arima, A. Asamitsu, G. Kido and N. Furukawa, Giant Magnetotransport Phenomena in Filling-Controlled Kondo Lattice System:  $\text{La}_{1-x}\text{Sr}_x\text{MnO}_3$ , J. Phys. Soc. Jpn. **63**, 3931 (1994).
  - [6] I. Terasaki, Y. Sasago, and K. Uchinokura, Large thermoelectric power in  $\text{NaCo}_2\text{O}_4$  single crystals, Phys. Rev. B **56**, R12685 (1997).
  - [7] Y. Maeno, H. Hashimoto, K. Yoshida, S. Nishizaki, T. Fujita, J. G. Bednorz, and F. Lichtenberg, Supercon-

- ductivity in a layered perovskite without copper, *Nature* **372**, 532 (1994).
- [8] K. Takada, H. Sakurai, E. Takayama-Muromachi, F. Izumi, R. A. Dilanian, and T. Sasaki, Superconductivity in two-dimensional  $\text{CoO}_2$  layers, *Nature* **422**, 53 (2003).
- [9] Y. Kamihara, T. Watanabe, M. Hirano, and H. Hosono, Iron-Based Layered Superconductor  $\text{La}[\text{O}_{1-x}\text{F}_x]\text{FeAs}$  ( $x = 0.05 - 0.12$ ) with  $T_c = 26$  K, *J. Am. Chem. Soc.* **130**, 3296 (2008).
- [10] T. Kimura, T. Goto, H. Shintani, K. Ishizaka, T. Arima, and Y. Tokura, Magnetic control of ferroelectric polarization, *Nature* **426**, 55 (2003).
- [11] B. J. Kim, H. Ohsumi, T. Komesu, S. Sakai, T. Morita, H. Takagi, and T. Arima, Phase-Sensitive Observation of a Spin-Orbital Mott State in  $\text{Sr}_2\text{IrO}_4$ , *Science* **323**, 1329 (2009).
- [12] K. Kitagawa, T. Takayama, Y. Matsumoto, A. Kato, R. Takano, Y. Kishimoto, S. Bette, R. Dinnebier, G. Jackeli, and H. Takagi, A spin-orbital-entangled quantum liquid on a honeycomb lattice, *Nature* **554**, 341 (2018).
- [13] T. Ohtsuki, Z. Tian, A. Endo, M. Halim, S. Katsumoto, Y. Kohama, K. Kindo, M. Lippmaa, and S. Nakatsuji, Strain-induced spontaneous Hall effect in an epitaxial thin film of a Luttinger semimetal, *Proc. Natl. Acad. Sci. USA* **116**, 8803 (2019).
- [14] M. Imada, A. Fujimori, and Y. Tokura, Metal-insulator transitions, *Rev. Mod. Phys.* **70**, 1039 (1998).
- [15] J. Hubbard, Electron Correlations in Narrow Energy Bands, *Proc. Royal Soc. A* **276**, 238 (1963).
- [16] A. Georges, G. Kotliar, W. Krauth, and M. J. Rozenberg, Dynamical mean-field theory of strongly correlated fermion systems and the limit of infinite dimensions, *Rev. Mod. Phys.* **68**, 13 (1996).
- [17] G. D. Mahan, Good Thermoelectrics, *Solid State Phys.* **51**, 81 (1998).
- [18] R. R. Heikes and R. W. Ure: *Thermoelectricity: Science and Engineering*, (Interscience Publishers, New York-London, 1961).
- [19] P. M. Chaikin and G. Beni, Thermopower in the correlated hopping regime, *Phys. Rev. B* **13**, 647 (1976).
- [20] J. -P. Doumerc, Thermoelectric Power for Carriers in Localized States: a Generalization of Heikes and Chaikin-Beni Formulae. *J. Solid State Chem.* **110**, 419 (1994).
- [21] D. B. Marsh and P. E. Parris, Theory of the Seebeck coefficient in  $\text{LaCrO}_3$  and related perovskite systems, *Phys. Rev. B* **54**, 7720 (1996).
- [22] D. B. Marsh and P. E. Parris, High-temperature thermopower of  $\text{LaMnO}_3$  and related systems, *Phys. Rev. B* **54**, 16602 (1996).
- [23] W. Koshibae, K. Tsutsui, and S. Maekawa, Thermopower in cobalt oxides, *Phys. Rev. B* **62**, 6869 (2000).
- [24] B. N. Figgis and M. A. Hitchman, *Ligand field theory and its applications* (Wiley, New York, 2000).
- [25] Y. Tanabe and S. Sugano, On the absorption spectra of complex ions I, *J. Phys. Soc. Jpn.* **9**, 753 (1954).
- [26] Y. Tanabe and S. Sugano, On the absorption spectra of complex ions II, *J. Phys. Soc. Jpn.* **9**, 766 (1954).
- [27] J. S. Griffith, *The theory of transition-metal ions* (Cambridge university press, London, 1971).
- [28] D. J. Singh, Electronic structure of  $\text{NaCO}_2\text{O}_4$ , *Phys. Rev. B* **61**, 13397 (2000).
- [29] R. Kubo, Statistical-Mechanical Theory of Irreversible Processes. I. General Theory and Simple Applications to Magnetic and Conduction Problems, *J. Phys. Soc. Jpn.* **12**, 570 (1957).
- [30] J. M. Luttinger, Theory of Thermal Transport Coefficients, *Phys. Rev.* **135**, A1505 (1964).
- [31] H. Matsuura, H. Maebashi, M. Ogata, and H. Fukuyama, Effect of Phonon Drag on Seebeck Coefficient Based on Linear Response Theory: Application to  $\text{FeSb}_2$ , *J. Phys. Soc. Jpn.* **88**, 074601 (2019).
- [32] W. Koshibae and S. Maekawa, Effects of spin and orbital degeneracy on the thermopower of strongly correlated systems, *Phys. Rev. Lett.* **87**, 236603 (2001).
- [33] M. M. Zemljic and P. Prelovsek, Thermoelectric power in one-dimensional Hubbard model, *Phys. Rev. B* **71**, 085110 (2005).
- [34] T. Okuda, K. Nakanishi, S. Miyasaka, and Y. Tokura, Large thermoelectric response of metallic perovskites:  $\text{La}_{1-x}\text{Sr}_x\text{TiO}_3$  ( $0 \leq x \leq 0.1$ ), *Phys. Rev. B* **63**, 113104 (2001).
- [35] A. V. Kovalevsky, A. A. Yaremchenko, S. Populoh, A. Weidenkaff, and J. R. Frade, Enhancement of thermoelectric performance in strontium titanate by praseodymium substitution, *J. Appl. Phys.* **113**, 053704 (2013).
- [36] M. Uchida, K. Oishi, M. Matsuo, W. Koshibae, Y. Onose, M. Mori, J. Fujioka, S. Miyasaka, S. Maekawa, and Y. Tokura, Thermoelectric response in the incoherent transport region near Mott transition: The case study of  $\text{La}_{1-x}\text{Sr}_x\text{VO}_3$ , *Phys. Rev. B* **83**, 165127 (2011).
- [37] D. P. Karim, and A. T. Aldred, Localized level hopping transport in  $\text{La}(\text{Sr})\text{CrO}_3$ , *Phys. Rev. B* **20**, 2255 (1979).
- [38] S. Pal, S. Hébert, C. Yaicle, C. Martin, and A. Maignan, Transport and magnetic properties of  $\text{Pr}_{1-x}\text{Ca}_x\text{CrO}_3$  ( $x = 0.0 - 0.5$ ): effect of  $t_{2g}$  orbital degeneracy on the thermoelectric power, *Eur. Phys. J. B* **53**, 5 (2006).
- [39] T. T. M. Palstra, A. P. Ramirez, S-W. Cheong, B. R. Zegarski, P. Schiffer, and J. Zaanen, Transport mechanisms in doped  $\text{LaMnO}_3$ : Evidence for polaron formation, *Phys. Rev. B* **56**, 5104 (1997).
- [40] W. Kobayashi, I. Terasaki, M. Mikami, and R. Funahashi, Negative thermoelectric power induced by positive carriers in  $\text{CaMn}_{3-x}\text{Cu}_x\text{Mn}_4\text{O}_{12}$ , *J. Phys. Soc. Jpn.* **73**, 523 (2004).
- [41] J. Mizusaki, T. Sasamoto, W. R. Cannon, and H. K. Bowen, Electric conductivity, Seebeck coefficient, and defect structure of  $\text{La}_{1-x}\text{Sr}_x\text{FeO}_3$  ( $x = 0.1, 0.25$ ), *J. Am. Ceram. Soc.* **66**, 247 (1983).
- [42] K. Berggold, M. Kriener, C. Zobel, A. Reichl, M. Reuther, R. Müller, A. Freimuth, and T. Lorenz, Thermal conductivity, thermopower, and figure of merit of  $\text{La}_{1-x}\text{Sr}_x\text{CoO}_3$ , *Phys. Rev. B* **72**, 155116 (2005).
- [43] Yang Wang, Yu Sui, Peng Ren, Lan Wang, Xianjie Wang, Wenhui Su, and Hong Jin Fan, Correlation between the structural distortions and thermoelectric characteristics in  $\text{La}_{1-x}\text{A}_x\text{CoO}_3$  ( $\text{A} = \text{Ca}$  and  $\text{Sr}$ ), *Inorg. Chem.* **49**, 3216 (2010).